

Regional scale modelling of meteorology and CO₂ for the Cabauw tall tower, The Netherlands

L.F. Tolk¹
W. Peters²
A.G.C.A. Meesters¹
M. Groenendijk¹
A.T. Vermeulen³

G.J. Steeneveld²

G.J. Steeneveld A.J. Dolman¹

¹VU University Amsterdam, Amsterdam, The Netherlands ²Wageningen University and Research Centre, Wageningen, The Netherlands ³Energy Research Centre of the Netherlands, Petten, The Netherlands

Published in Biogeosciences Discuss., 6, 5891-5931, 2009

ECN-W--09-016 JUNE 2009

Biogeosciences Discuss., 6, 5891–5931, 2009 www.biogeosciences-discuss.net/6/5891/2009/ © Author(s) 2009. This work is distributed under the Creative Commons Attribution 3.0 License.



Biogeosciences Discussions is the access reviewed discussion forum of Biogeosciences

Regional scale modelling of meteorology and CO₂ for the Cabauw tall tower, The Netherlands

L. F. Tolk¹, W. Peters², A. G. C. A. Meesters¹, M. Groenendijk¹, A. T. Vermeulen³, G. J. Steeneveld², and A. J. Dolman¹

Received: 2 May 2009 - Accepted: 15 June 2009 - Published: 22 June 2009

Correspondence to: L. F. Tolk (lieselotte.tolk@falw.vu.nl)

Published by Copernicus Publications on behalf of the European Geosciences Union.

5891

Abstract

We simulated meteorology and atmospheric CO₂ transport over the Netherlands with the mesoscale model RAMS-Leaf3 coupled to the biospheric CO2 flux model 5PM. The results were compared with meteorological and CO₂ observations, with particular attention to the tall tower of Cabauw. An analysis of the coupled exchange of energy, moisture and CO₂ showed that the surface fluxes in the domain strongly influenced the atmospheric properties. The majority of the variability in the afternoon CO2 mixing ratio in the middle of the domain was determined by biospheric and fossil fuel CO2 fluxes in the limited area domain (640×640 km). Variation of the surface CO2 fluxes, reflecting the uncertainty of the parameters in the CO₂ flux model 5PM, resulted in a range of simulated atmospheric CO₂ mixing ratios of about 12 ppm in the well-mixed boundary layer. Additionally, we identified an uncertainty in the surface energy fluxes. The spread caused by this uncertainty in the simulated atmospheric vertical mixing caused a CO₂ transport error of 1.7 ppm. This is an important source of uncertainty and should be accounted for to avoid biased estimates of the CO2 mixing ratio, but does not overwhelm the signal in the CO₂ mixing ratio due to the spread in CO₂ surface fluxes.

1 Introduction

Terrestrial carbon uptake is an important process in the global carbon cycle. It removes a substantial part of the anthropogenic emitted CO₂ from the atmosphere (Canadell et al., 2007). A potentially useful method to increase our understanding of the terrestrial CO₂ fluxes is inverse modelling of atmospheric CO₂ mixing ratio observations (e.g. Gurney et al., 2002). In this approach the atmospheric signal is used to constrain the surface fluxes by the backward use of an atmospheric transport model. The results of such an inversion study depend to a large extent on the quality of atmospheric modelling (Stephens et al., 2007).

¹VU University Amsterdam, Amsterdam, The Netherlands

²Wageningen University and Research Centre, Wageningen, The Netherlands

³Energy Research Centre of the Netherlands, Petten, The Netherlands

Therefore, correct simulation of the atmospheric transport, and accounting for the uncertainties in it, is an important step towards inverse modelling of CO_2 . Atmospheric transport is modelled at increasing resolutions to capture the high spatial and temporal variability in the CO_2 mixing ratios over the continent. Continental scale studies showed that the forward simulation of CO_2 improved by increasing the horizontal resolution from a number of degrees (Gurney et al., 2002) to about one degree or less (Geels et al., 2007; Parazoo et al., 2008). Further increasing the horizontal resolution to just a few kilometres in more limited domain studies (Dolman et al., 2006) was shown to improve the CO_2 mixing ratio simulation at observation stations in uneven and coastal terrain, because of their ability to simulate mesoscale circulations, like sea breezes and katabatic flows (Nicholls et al., 2004; Riley et al., 2005; Van der Molen and Dolman, 2007; Sarrat et al., 2007; Ahmadov et al., 2009) and to avoid representation errors by resolving a larger part of the variability in the CO_2 mixing ratio (Corbin et al., 2008; Tolk et al., 2008).

Despite these achievements correct modelling of the CO_2 mixing ratios remains challenging. Model intercomparisons of global (Stephens et al., 2007; Law et al., 2008), continental (Geels et al., 2007) and mesoscale models (Van Lipzig et al., 2006; Sarrat et al., 2007) showed some discrepancies in the meteorology and CO_2 modelled between different models. In the simulation of CO_2 mixing ratios both advection and entrainment play an important role (Vila et al., 2004; Casso-Torralba et al., 2008) and the quantification of uncertainties in these physical processes is one of the major questions in transport modelling. Comparisons with observations showed that an erroneous simulation of the advection (Lin and Gerbig, 2005) and vertical mixing (Gerbig et al., 2008) can lead to uncertainties in the simulated CO_2 mixing ratio of several ppm.

In the present study a high resolution simulation is performed with the non-hydrostatic Regional Atmospheric Modeling System (RAMS; Pielke et al., 1992). The performance of the simulation is validated with meteorological and CO₂ observations. We address a potential source of error in the simulated atmospheric vertical mixing: the simulation of the surface energy fluxes. Its uncertainty is estimated based on a

5893

comparison of results obtained with different models (RAMS, WRF and ECMWF) and different model settings within RAMS, with both surface flux and atmospheric observations.

We coupled the biospheric CO_2 flux model 5PM to the RAMS atmospheric transport model, in order to study the coupled exchange of energy, moisture and CO_2 . In this framework the impact of the surface energy fluxes on the simulation of vertical atmospheric mixing and consequently on the CO_2 mixing ratio is quantified. Novel in our approach is that we distillate the impact of the uncertainty in the simulated surface energy fluxes on the atmospheric CO_2 mixing ratio, and that we quantify this CO_2 transport error in a Eulerian approach.

Also, the uncertainty in the CO_2 surface fluxes is addressed. With the coupled RAMS-5PM simulation system these are propagated into a range of CO_2 mixing ratios. This indicates the minimal performance of the atmospheric transport model required for the use in inversion studies, since the uncertainty in the transport modelling should not exceed the uncertainty related to CO_2 surface flux uncertainty. The parameters in the biospheric model 5PM have been optimized in a previous study for a number of eddy correlation flux observations (Groenendijk et al., 2009). Innovative in this study is that we show at mesoscale a realistic uncertainty range of CO_2 mixing ratios due to uncertainties in the CO_2 surface fluxes, based on independently determined a-priori flux estimates.

Finally, we separate the contribution of different CO_2 sources and sinks to the CO_2 mixing ratio at Cabauw, i.e. the influence of the global background, fossil fuel, sea, respiration and assimilation fluxes. The relative importance of the different CO_2 sources and sinks indicates which uncertainties in the surface CO_2 fluxes are important and which can be neglected. Additionally, in this way the relative contribution of the near field versus the far field fluxes on the CO_2 mixing ratio is shown, another important subject in regional scale inverse modelling (Zupanski et al., 2007; Lauvaux et al., 2008; Gerbig et al., 2009). Overall, we aim to provide a solid basis for future inversion studies at a regional scale, amongst others for the area at scope here.

The remainder of the paper is organized as follows: in Sect. 2 the simulation set-up is described, in Sect. 3 the performance of the model is validated against meteorological observations, Sect. 4 describes the simulated $\rm CO_2$ fluxes and mixing ratios in comparison with observations and in Sect. 5 the implications of our results for the interpretation of the observations, future forward and inverse $\rm CO_2$ simulations are discussed.

2 Methods

2.1 Simulation period and domain

We performed simulations with the Regional Atmospheric Modeling System (RAMS) for 22 days in June 2006. In this part of the year the biogenic assimilation fluxes during daytime of CO_2 were relatively large. This period was selected because it covered a number of meteorological regimes with different wind directions and frontal passages, influencing the atmospheric properties and carbon exchange. South-easterly winds coincided with clear sky conditions, while northerly and south-westerly winds caused more cloudy conditions.

A two way nested grid was used (Fig. 1) centred on the Netherlands at 52.25° N and 5.2° E, with a 320×320 km domain at 4 km resolution nested in a 640×640 km domain at 16 km resolution (Table 1). The dominant land use types in the area are cultivated lands (crops and grasslands) and urban built up. Large cities and industrial areas of the Netherlands, Belgium and the German Ruhr Area can be found within the domain. To the north and the west the Netherlands is bounded by the North Sea.

2.2 Simulation setup

The atmospheric simulations were performed with the non-hydrostatic mesoscale model RAMS (Pielke et al., 1992), which has already been used to simulate the behaviour of CO₂ in the atmosphere in a number of studies (e.g. Denning et al., 2003;

5895

Nicholls et al., 2004; Sarrat et al., 2007; Ter Maat and Hutjes, 2008). The version used in this study is B-RAMS-3.2, including adaptations to secure mass conservation (Medvigy et al., 2005; Meesters et al., 2008). We extended RAMS with the medium range forecast (MRF) turbulence scheme, which has a non-local turbulence parameterization and was shown by Troen and Mahrt (1986), Holtslag et al. (1995) and Hong and Pan (1996) to simulate the daytime boundary layer structures more realistic than local mixing schemes. The surface energy fluxes were simulated using Leaf-3 (Walko et al., 2000).

Meteorology, soil temperature and soil moisture were initialized with ECMWF analysis data (Uppala et al., 2005). In order to be consistent with the RAMS soil wilting point (wp) and field capacity (fc), the ECMWF soil moisture (η) was scaled towards RAMS soil variables based on a soil wetness index (SWI):

$$SWI = \frac{\eta - \eta_{wp}}{\eta_{fc} - \eta_{wp}} \tag{1}$$

$$\eta_{\text{RAMS}} = \eta_{wp,\text{RAMS}} + \text{SWI}_{\text{ECMWF}} \left(\eta_{fc,\text{RAMS}} - \eta_{wp,\text{RAMS}} \right)$$
(2)

CarbonTracker optimized CO₂ mixing ratio fields at 1×1° resolution (Peters et al., 2007) were used for initialization and boundary conditions of the CO₂ mixing ratio. The simulations were nudged every 3 h to CarbonTracker CO₂ mixing ratios and every 6 h to the ECMWF analysis meteorology with a nudging relaxation time scale of 900 s. The nudging extended inward from the lateral boundary by 5 grid cells and the centre of the domain was free of nudging.

2.3 CO₂ fluxes

 CO_2 fluxes from fossil fuel burning were included in the simulations based on the IER database at 10 km resolution (www.carboeurope.ier.uni-stuttgart.de). The CO_2 fluxes from the coastal sea inside the domain were calculated based on climatologic estimates of the partial pressure of CO_2 in the sea (Wanninkhof, 1992; Takahashi et al.,

2002). Biospheric CO_2 surface fluxes were modelled with 5PM (Groenendijk et al., 2009). This model was coupled to RAMS through the radiation, the temperature and humidity of the canopy air and influences the CO_2 mixing ratio at the lowest atmospheric level. The CO_2 assimilation does not depend on the energy fluxes of RAMS through the stomatal conductance (Collatz et al., 1991). In 5PM the photosynthesis is determined following Farquhar et al. (1980), where photosynthesis is either limited by the carboxylation rate, which is enzyme limited, or by the light limited RuBP regeneration rate. The most important assimilation parameters in this model are the maximum carboxylation capacity (Vc_{max}) and the light use efficiency (α). Respiration was calculated with the relationship by Lloyd and Taylor (1994):

$$R = R_{10} e^{\frac{E_0}{\Re} \left(\frac{1}{283.15 - T_0} - \frac{1}{T - T_0} \right)}$$
 (3)

where R_{10} is the respiration rate at a reference temperature of 10°C, $\frac{E_0}{\Re}$ is the activation energy divided by the universal gas constant, T_0 is a constant of 227.13 K and T is soil temperature. For further specifications of 5PM see Groenendijk et al. (2009).

Groenendijk et al. (2009) optimized the parameters of this model (Vc_{max} , α , R_{10} and E_0) for the full canopy based on a large number of Fluxnet observations (Baldocchi et al., 2001). We applied parameter values optimized for the temperate zone, for the period of May–July for all years (Table 2). Simulations were performed with CO_2 fluxes calculated based on the best guess parameter values. For respiration and assimilation of the most abundant vegetation species (crops and grass) we also simulated fluxes using the upper and the lower parameter values within the standard deviation of the parameter estimate. In this way a range of CO_2 mixing ratios was simulated based on the different CO_2 flux parameter settings.

Each CO_2 mixing ratio signal, i.e. from the global background, fossil fuel fluxes, sea fluxes and the different fluxes of respiration and assimilation, was simulated as a separate atmospheric tracer. The total CO_2 mixing ratio is the sum of these separate tracers. This enabled us to distinguish between the influence of the different components on the CO_2 mixing ratio. Further specifications on the design of the simulations

are given in Table 1.

2.4 Observations

A large number of number of observations of the atmospheric properties and the surface fluxes were available for model validation. Data from continuous $\rm CO_2$ mixing ratio measurements, performed by a Licor 7000 with a precision of 0.05 ppm, and meteorological data from the tall tower at Cabauw at a height of 20 m, 60 m, 120 m and 200 m were used. Also, atmospheric observations for temperature, humidity, wind speed and direction were available at 110 synoptic 2 m stations over the Netherlands and from the radiosondes that were released twice a day at De Bilt, which is about 25 km north-east of the Cabauw site. Observations of the surface fluxes were available for sensible heat, latent heat and $\rm CO_2$ fluxes from eddy correlation measurements (Aubinet et al., 2001; Dolman et al., 2002; Wilson et al., 2002; Jacobs et al., 2007; Braam, 2008; Aubinet et al., 2009). Additionally, scintillometer measurements provided extra sensible heat flux measurements over a horizontal path of 0.35–5 km (De Bruin et al., 2004). The locations are specified in Fig. 1 and in Table 3.

3 Results: meteorological performance of the model

3.1 Consistency of the simulation in time

The simulated period of 22 days covered a number of different weather regimes with different wind directions, solar radiation and temperature (Fig. 2). East to south-easterly winds brought clear weather, with increasing temperature and relative large day-night temperature amplitudes, like at 9–14 June 2006 (doy 160–165). In general, northern and south-westerly winds brought more cloudy conditions with reduced radiation, lower temperatures and smaller nocturnal cooling.

Here we show the results of the standard simulation used in this study. For this simulation, the standard RAMS settings have been modified to obtain a more realistic

Bowen ratio, as will be expounded in Sect. 3.2. The model reproduced the synoptic variations over the full 22-day period without any explicit re-initialization of the simulation (Fig. 2 and Table 4). This was achieved by prescribing analyzed meteorological boundary conditions. A change in the large-scale atmospheric situation was thus passed on to the inner domain for which RAMS simulated, mimicking the effect of a re-initialization. A large advantage of not needing to re-initialize the RAMS model over multi-week periods is that mass continuity of tracers and a balance of the physical equations for energy and water was ensured.

A comparison of the statistics for the first and last half of the period showed the consistency of the model performance in time (Table 4). Hourly temperature (*T*) and humidity (*q*) were simulated comparably well in both periods. Radiation showed a better performance in the first half of the period, that can be attributed to the occurrence of clouds in the second half of the period, rather than to a drift of the simulated meteorology with time. Incoming solar radiation and its reduction by clouds was mostly simulated with the correct amplitude and frequency. However, the exact location of the clouds and subsequently the timing of the radiation reduction sometimes deviated from the observations, as was also seen in similar mesoscale model studies (Denning et al., 2003; Van Lipzig et al., 2006; Parazoo et al., 2008).

3.2 Uncertainties in the surface energy fluxes

Surface energy fluxes are important drivers of processes in the atmosphere, influencing e.g. atmospheric \mathcal{T},q and vertical mixing. Uncertainties in the surface energy fluxes thus may be an important source of uncertainty in the simulation of the atmospheric properties and are addressed in this section.

We compared the simulated energy fluxes with eddy covariance and scintillometer measurements (Fig. 3) and made a comparison with two other models: WRF and ECMWF. Additionally, we studied the sensitivity of the simulated sensible (H) and latent (LE) heat fluxes to changes in the surface flux calculation by Leaf3, and its effect on the atmosphere. This revealed that the simulations at some days either correctly captured

5899

the observed surface energy fluxes, or the observed T and q vertical profile in the planetary boundary layer (PBL), but could not reconcile both at the same time. The results of the sensitivity tests are shown in Table 5 and described below, with a focus on T and H because of their importance for atmospheric vertical mixing.

The energy fluxes showed a large variation between low (crops, grasslands) and high (forest) vegetation types (Fig. 3, note the different scale on the y-axis for low and high vegetation). These differences were driven by differing vegetation characteristics such as the low aerodynamic resistance and stomatal conductance in forest and were reproduced in the RAMS simulations.

With the standard Leaf3 vegetation characteristics (green line in Fig. 3) most of the eddy correlation observations were captured reasonably well. The scintillometer observations at Maas-en-Waal and Haarweg were slightly underestimated. With these settings the PBL *T* was underestimated and *q* overestimated at clear days with eastern winds, in comparison with radiosonde observations (Fig. 4 and Table 5), the Cabauw tall tower and synoptic 2 m observations (not shown).

We compared our findings with the ECMWF (Uppala et al., 2005) forecast simulations and with a simulation performed with WRF (Skamarock et al., 2008) using the MRF PBL scheme and either ECMWF or NCEP boundary conditions for the same domain and period. Both simulations matched the observed T well (not shown), but also failed to match the observed H for grass and crops (light and dark blue lines in Fig. 3).

Sensitivity tests showed that the strength of LE and H depended strongly on (1) the water availability, (2) the minimal stomatal resistance, which determines the plants' resistance to transport of water and CO_2 and (3) the fraction of the surface that is vegetated (Table 5).

(1) Decreasing the soil moisture content led to a strong increase in the Bowen ratio (i.e. the ratio of sensible to latent heat flux, β) because of the decrease in evaporation from the soil and transpiration from the plants. (2) Also a doubling of the minimal stomatal resistance, a rather uncertain parameter in Leaf3 (Walko et al., 2000), for grass and crops from $100\,\mathrm{sm}^{-1}$ to $200\,\mathrm{sm}^{-1}$ increased β . (3) With standard Leaf3

settings the vegetation fraction of grass and crops did not exceed ~70%, even with a high LAI. We increased the vegetation fraction to 90% when the LAI is larger than 1, in line with for example the settings in the ECMWF surface model. This increase led to a considerable increase in H and the atmospheric T (Table 5). Simulations with these adapted settings returned an overestimation of H at most of the low vegetation sites (e.g. with adaptations (2) and (3), red line in Fig. 3), but returned a rather well simulated PBL T and T (red lines in Figs. 2 and 4). We will refer to the simulation with increased stomatal resistance and vegetation fraction and standard soil moisture as the "high T simulation", while the simulation with standard Leaf3 vegetation characteristics will be referred to as the "low T simulation".

We tested the sensitivity of our findings to the moment of initialization. When initialized 6 h, 18 h or over 5 days in advance, the simulated noon temperatures deviated 2.0, 2.5 or 3.1 K from the observations, respectively (Table 5) using the settings yielding the low β . Hence, the largest part of the temperature underestimation built up within a few hours and was rather independent of the moment of initialization. For the high β simulation the results were robust to a change of the moment of initialization (not shown).

The difference in the simulated β by ECMWF, WRF and RAMS, and the different optimal Leaf3 model settings suggested by atmospheric and surface observations, indicate an uncertainty in the correct β for the full domain. Further discussion on this will be presented in Sect. 5. We will use the simulation with the high β (and hence lowest T and q bias in the atmosphere) to investigate the structure of the simulated CO₂ fields. This simulation corresponds to the standard run that was discussed in Sect. 3.1. In the next section the effects of the uncertainty in the surface energy fluxes on the atmospheric vertical mixing are addressed.

3.3 Atmospheric temperature and humidity profiles

The results of the simulations with (1) low β and (2) high β were compared with the radiosonde observations in De Bilt (e.g. Fig. 4). Generally a well-mixed PBL developed 5901

that has a lower potential temperature and is moister than the free troposphere. At clear nights cooling near the surface led to a shallow (200 m) and stable PBL.

Simulations with the MRF turbulence scheme showed a better performance than the standard RAMS Mellor Yamada turbulence scheme (Fig. 4). Still, the height of the PBL was not always captured correctly and the jump of T and q was less sharp than observed. Increasing the vertical resolution to 60 instead of 25 vertical layers in the lower 3 km of the atmosphere did not change this. This is likely due to uncertainties in the parameterization of vertical transport, like lack of subsidence, too much entrainment or an incorrect free tropospheric lapse rate of T or q. Improvements in the available PBL schemes would be needed to improve the simulation of these processes. The free tropospheric values are generally assumed reasonable due to the use of ECMWF analysis boundary conditions.

Simulation of the nocturnal PBL is even more challenging. The atmospheric stability during clear nights was systematically underestimated by the model, which is a common feature for most atmospheric transport models (Geels et al., 2007; Gerbig et al., 2008). In the simulation the nocturnal surface signal reached up to $\sim\!400\,\mathrm{m}$ while in the observations it was limited to $\sim\!200\,\mathrm{m}$. This inaccurately simulated height of the PBL will cause discrepancies in the mixing ratios which are not directly related to the CO₂ fluxes.

The depth of the PBL is amongst others driven by the surface sensible heat fluxes. Uncertainty in these, as described in Sect. 3.2, may thus reflect in uncertainties in the PBL depth. At days when the PBL height was clearly defined the root-mean-square error (RMSE) of the noon PBL height was for both simulations ~ 350 m. The simulation with a relative low β (1, green line in Fig. 4) showed a mean bias of ~ -100 m, while the simulation with a higher β (2, red line in Fig. 4) had a positive mean bias of ~ 75 m. The uncertainty in the surface fluxes thus clearly influenced the atmospheric mixing ratio and can explain a part of the uncertainty in the simulated PBL height as for example indicated for ECMWF simulations in Gerbig et al. (2008).

4 Results: CO₂ fluxes and mixing ratios

The framework of the simulated meteorology as described in the previous sections allows us to study the coupling between the surface CO_2 fluxes and the atmospheric CO_2 mixing ratios. First, we will address the uncertainties in the CO_2 fluxes. Secondly, we will show how these propagate into a range of simulated CO_2 mixing ratios which is compared to the observations at the Cabauw tall tower. Finally, the contribution of the different CO_2 fluxes and the background CO_2 to the total CO_2 mixing ratio is unravelled.

4.1 CO₂ flux variability

The CO_2 fluxes and mixing ratios were simulated with the coupled model RAMS-5PM with parameter settings based on optimizations by Groenendijk et al. (2009); see methods Sect. 2.3. The optimized parameters showed a rather large variability in time and space. This causes an uncertainty in the average CO_2 flux parameter values (Table 2). The unresolved variability in the CO_2 fluxes is illustrated here with observations at four locations in the domain (Fig. 5).

The shown simulated CO_2 fluxes were calculated with the parameters that gave an unbiased result compared to the observed CO_2 mixing ratio at 200 m at Cabauw. The selected parameter values are indicated in brackets in Table 2. Note that in a follow-up study we intend to formally estimate the parameters of the 5PM model based on the forward results presented here, rather than simply selecting an unbiased set of values.

Respiration fluxes show a soil temperature driven diurnal and synoptic variation, which is represented by the model (Fig. 5a). Besides, the observed respiration fluxes also showed differences between sites, not observed in *T* and not included in the model. For example, with the same parameter settings, the observed respiration fluxes in Lonzee were captured, but were systematically overestimated for another crops site: Lutjewad. Grass sites (Cabauw and Horstermeer) showed variations mainly in the diurnal amplitude of the respiration. Jacobs et al. (2007) showed that the variation of the respiration of grass sites within the Netherlands is mainly due to the difference be-

5903

tween organic and mineral soils. The soil map underlying this simulation lacks this kind of detail, hampering the simulation of variation within the respiration fluxes.

Assimilation fluxes were inhomogeneous in space and time as well (Fig. 5b). Generally, the uptake by crops was higher than by grass, as was correctly simulated. Also the observed assimilation reduction at days with limited radiation was captured by the model (within the limitations of the RAMS radiation calculations). With the parameter settings selected based on the Cabauw atmospheric CO₂ concentrations, many observed assimilation fluxes were fairly well reproduced, e.g. for the grass sites and for the second half of the period at the crops site Lonzee.

Nonetheless, these same CO_2 flux parameter settings led to an underestimation of the CO_2 fluxes at Lutjewad with almost 30% and an overestimation of the fluxes at Lonzee in the beginning of the period, most probably due to vegetation growth. To overcome the latter the model must be extended with LAI (e.g. Sellers et al., 1996), this may also give a better representation of the spatial variability of the assimilation fluxes. Besides, differences in for example crops species and land management may explain the variability between Lonzee and Lutjewad. These were not resolved in the simulation, but included in the uncertainty range of the CO_2 assimilation parameters in 5PM (Table 2).

4.2 CO₂ mixing ratios

Uncertainties in the CO₂ respiration and assimilation fluxes had a significant influence on the CO₂ mixing ratio when terrestrial fluxes are in the footprint of the observation. The different CO₂ flux parameter settings returned a range of simulated CO₂ mixing ratios (Fig. 6). This range varied in time between 1 ppm and 25 ppm, with a mean of 11.7 ppm in the well mixed afternoon PBL (at 200 m height). Small ranges were related to northern or south-westerly wind directions (Fig. 2), when the air predominantly originated from over sea and the land signal is suppressed, while a broader range occurred when the continental signal was large, i.e. with south-easterly wind, low wind speeds or frontal passages. This broad range indicated that the atmospheric mixing ratio poten-

tially contained much information about the CO_2 fluxes within the simulation domain. This is in line with studies from Lauvaux et al. (2008) and Zupanski et al. (2007) and shows the potential for future inversion on this temporal and spatial scale.

However, the uncertainties in the simulation of the meteorology discussed in Sect. 3 give rise to uncertainties in the simulated CO_2 transport. Here we give an overview of the impact of those features on the simulation of the CO_2 mixing ratios.

The uncertainty in the surface energy fluxes (Sect. 3.2) and consequently the vertical mixing (Sect. 3.3) results in an uncertainty in the CO_2 mixing ratio. To quantify this the results of the simulations with relative low (1) and high (2) simulated β , were compared for CO_2 (not shown). These two simulations (with the same CO_2 flux parameter settings) returned a difference in the afternoon CO_2 mixing ratio of on average 1.9 ppm. This was to a small extent due to changes in the respiration caused by the temperature difference (\sim 0.3 μ mol m⁻² s⁻¹ per K temperature change). Compensating for this by slightly adjusting the R_{10} left a difference of 1.7 ppm. This is the uncertainty in the CO_2 mixing ratio caused by the difference in vertical mixing due to the surface flux uncertainty.

Other difficulties were related to the simulation of the nocturnal CO_2 mixing ratio, which is up to now, because of the known large uncertainties in the transport model vertical mixing schemes in stable conditions, not used in inversion studies (Gurney et al., 2002; Stephens et al., 2007; Geels et al., 2007). Our simulations confirm that the simulation of nocturnal CO_2 is biased, because of the simulation of a too deep nocturnal PBL (see Sect. 3.3). The absolute nocturnal CO_2 mixing ratio accumulation was not simulated correctly, leading to a low R^2 of the CO_2 mixing ratio time series at 200 m (Table 4) and simulated mixing ratios at 60–200 m that were during some nights totally outside the range of simulated CO_2 mixing ratios. As such it is clear that the representation of the nocturnal boundary layer in mesoscale models requires improvement.

Nevertheless a significant part of the diurnal variations, especially at lower sample levels, is captured by simulations. During the nights CO₂ accumulates near the surface

5905

and mixing ratios of over 450 ppm were seen at 20 m (Fig. 6). In the morning the PBL became unstable and the signal of the lower layers was mixed onto higher levels. This was for example reflected by early morning peaks at 200 m height, in the observations as well as the simulations. During a number of nights a sudden drop of mixing ratios was seen in the mixing ratio at 20 and 60 m around midnight, this is most likely due to the formation of a low level jet (e.g. Bosveld et al., 2008) and represented in the simulations (for example at 11, 12 and 19; doy 162, 163 and 170). This shows the ability of the model to represent such stability changes at small temporal scales.

Another important source of uncertainty is the simulated location and the timing of the cloud cover (Sect. 3.1). At partly clouded days, this led to an error in simulation of the CO₂ fluxes and the depth of the PBL, and consequently biases in the CO₂ mixing ratio. Therefore, the exact simulated mixing ratios at these days should be regarded as more uncertain. Frontal passages may cause a comparable misrepresentation of the simulated concentrations (e.g. at 25 June; doy 176). Finally, a sudden concentration jump in the observations, for example at 10 June (doy 161; see Fig. 6) with almost 10 ppm in the well mixed PBL, is probably best explained as a fossil fuel plume missed by the model.

4.3 Different tracer signals at Cabauw

To study the relative importance of the different sources and sinks influencing the $\rm CO_2$ mixing ratios we disaggregated the simulated $\rm CO_2$ mixing ratios at Cabauw into contributions from (a) $\rm CO_2$ entering through the lateral boundaries (further called background concentration) and (b) fluxes from within the RAMS domain. The latter were further separated into contributions from assimilation and respiration of different vegetation types, sea fluxes and fossil fuel emissions, which were included in the simulation as separate atmospheric tracers (Figs. 7 and 8).

Assimilation and respiration fluxes were important in determining the CO_2 mixing ratio. They had an average influence during the day of -10.5 and 7.8 ppm respectively, with peaks up to ~ 30 ppm at 200 m (Figs. 7 and 8a). In the nocturnal PBL the respi-

ration tracer showed peaks up to ~60 ppm at 20 m (not shown). The total biosphere signal, i.e. the sum of the respiration and assimilation, was because of the cancelling opposite signs more modest and had an average influence of 3.2 ppm.

Generally, the crops tracer was the most abundant assimilation tracer, even though Cabauw is a grassland site (Fig. 8b). This was due to the relative high assimilation of crops compared to grass (Fig. 5b) combined with the rather large amount of crops in the domain (Fig. 1). In the Pelcom land use map the amount of crops may be overestimated. Nonetheless this shows that at both 20 m and 200 m the local vegetation type did not give the largest assimilation signal during the day in the well-mixed PBL.

In our domain the fossil fuel was also an important contributor to the total signal. Plumes with high fossil fuel tracer concentrations originating from the industrial sources moved over the domain. The major sources were the Ruhr Area, southeast of the Netherlands, the ports in the southwest of the Netherlands and in Belgium, and smaller diffuse sources found over the total domain. Afternoon values in the well mixed PBL varied between 2–8 ppm and the average mixing ratio of the fossil fuel fluxes was almost as large as the biospheric signal whereas its afternoon variance is half that of the biospheric signal (Fig. 8c).

The contribution of the sea fluxes to the total signal was at these timescales very limited (Figs. 8a and c). Although on a global scale the assimilation of CO_2 by the oceans plays an important role, here its influence was small because of the limited timeframe and the relatively small area. The average flux of $\sim 0.02 \, \mu \text{mol} \, \text{m}^{-2} \, \text{s}^{-1}$ at the North Sea was negligible compared to the continental fluxes in the domain.

 ${\rm CO_2}$ mixing ratios entering the domain through the lateral boundaries showed a strong diurnal cycle over land, and a much smaller cycle over the sea. When the wind direction was steady from the east or south the low daily continental values in the background mixing ratio, caused by assimilation over the continent outside of our simulation domain, reached Cabauw. This was for example seen at 12 and 13 June (doy 163 and 164) when the background concentration was reduced by ~10 ppm. Because the influence on the mixing ratios in the middle of the domain can be considerable, the quality

5907

of the boundary conditions in a limited domain simulation is important.

5 Discussion and conclusions

We simulated three weeks in June 2006 with the B-RAMS-3.2 mesoscale model at 4km resolution. The simulations were able to reproduce the observed time series of the meteorological variables and CO_2 mixing ratios satisfactorily for most of the three week period. The model performance showed no drift and comparison with data remained acceptable throughout the full simulation. We found only limited sensitivity of the model performance to the moment of initialization. This, combined with the absence of significant drift, shows the possibility of a non-stop simulation without divergence of the results from the observations. Hence, in our simulations a re-initialization of the meteorology does not seem necessary. The advection of the nudged ECMWF meteorological and CarbonTracker CO_2 mixing ratio boundary conditions over the domain prevents a runaway of the results in a dynamical and continuous way.

The simulations with the newly in RAMS implemented MRF scheme showed a better performance than the standard Mellor Yamada scheme. This is in line with the findings of Holtslag et al. (1995) for the Dutch situation and confirms the importance of the parameterizations of turbulence and entrainment (Vila et al., 2004; Casso-Torralba et al., 2008) for the simulation of the atmospheric profiles.

Also a realistic simulation of surface energy fluxes is important for the simulation of the atmospheric vertical mixing. Comparison with other models (WRF, ECMWF) and observations revealed a discrepancy between the simulations and the surface observations on the one hand and the atmospheric observations on the other hand. For a number of days the observed *T* profile could not be reconciled with *H* observations, something also seen in previous studies (e.g. Holtslag et al., 1995; Ek and Holtslag, 2004). Besides, the observed PBL height could at those days not be reproduced with a simple mixed layer model (Vila and Casso-Torralba, 2007) based on the observed *H*. It suggests that the total Bowen ratio (β) over the full domain may be higher than

indicated by the surface observations and thus reveals an uncertainty in the surface fluxes. This may be due to heterogeneity of the fluxes within one vegetation type (e.g. Baldocchi et al., 2001) which is not included in our land surface scheme. Also, the limited amount of observations over grass and crops, especially in the eastern part of the domain, and energy balance closure problems (Wilson et al., 2002) of e.g. ~30% for the Cabauw surface flux observations (Braam, 2008) may add uncertainty to the total surface flux estimate over the domain. Moreover, (freestanding) houses, trees and roads may lead to a different domain averaged β than observed with the surface observations over vegetated terrain only.

The uncertainty in the sensible heat flux adds uncertainty to the simulation of the PBL height. A comparison of simulations with a relative low β (confirmed by the surface observations) and relative high β (suggested by atmospheric observations and the ECMWF and WRF simulations) was made. This led to a difference in the noon PBL height of ~22%. A comparable sensitivity of the PBL height to changes in the surface energy fluxes (20%) was found by Vila and Casso-Torralba (2007) in a simple mixed layer study for Cabauw.

The surface energy flux and the resulting PBL height uncertainty caused a difference in the simulated $\rm CO_2$ mixing ratio of ~1.7 ppm. This is in the same order of magnitude as other $\rm CO_2$ transport errors, such as representation (0.5–3 ppm; Van der Molen and Dolman, 2007; Tolk et al., 2008) and advection (~5 ppm; Lin and Gerbig, 2005) errors, and much larger than the measurement accuracy. It may explain about half of the 3.5 ppm uncertainty due to errors in the PBL height estimated by Gerbig et al. (2008). To avoid biased $\rm CO_2$ mixing ratio estimates, a comparison with observations of the simulated PBL height and, if needed, adjustment of the surface fluxes like described in Sect. 3.2 is recommended as first step in an inversion.

The surface CO₂ fluxes in the domain strongly influenced the simulated CO₂ mixing ratios at Cabauw, causing by far the most of afternoon CO₂ mixing ratio variability (Fig. 8c). A realistic variation of parameter settings for the calculation of CO₂ fluxes (Groenendijk et al., 2009) resulted in a range of simulated CO₂ mixing ratios of

5909

11.7 ppm. This atmospheric signal will in future inversion studies be used to constrain the surface CO_2 fluxes. The rather broad range indicates the potential for inversions, even though transport errors are in the order of several ppm. It confirms, with a complementary approach, the findings of Lin and Gerbig (2005) and Gerbig et al. (2008) and is in line with previous studies that stress the importance of the near field fluxes for the CO_2 mixing ratios over the continent (Zupanski et al., 2007; Lauvaux et al., 2008; Gerbig et al., 2009).

Although grass is the dominant vegetation type near Cabauw (Fig. 1) its atmospheric CO₂ mixing ratio is strongly affected by the assimilation of crops. This is due to the large magnitude of crops assimilation, the large area covered with crops, advection of the atmospheric signal and at wind still days entrainment from the residual boundary layer (Casso-Torralba et al., 2008; Vila et al., 2004). Hence, the information in the atmospheric mixing ratio measurements is not limited to the very local fluxes within the nearest tens of kilometres. We conclude therefore that the scale of tens to hundreds of kilometers is convenient for future inversions of the atmospheric CO₂ mixing ratio signal at the tall tower of Cabauw.

Another important contributor to the CO_2 mixing ratio at Cabauw are the fossil fuel CO_2 fluxes. At these small scales uncertainties in the timing and exact location of the fluxes are important. The general assumption in global inversions that the fossil fuel fluxes are well known (Gurney et al., 2002) may be true for aggregated values in space and time (annual country totals) but is certainly not true for the scales in time and space that are modeled here. Because of the relative importance of the fossil fuel atmospheric signal, uncertainties in the timing and magnitude fossil fuel fluxes should be taken into account in future regional inversion studies.

The grass and crops assimilation tracers as simulated for Cabauw have a rather high correlation coefficient (0.67). This may imply that the ability of the atmospheric signal to distinguish between vegetation types is limited. The respiration and assimilation flux signals cancel each other during the day (correlation = -0.80), providing a relatively modest cumulative atmospheric signal that may not constrain the two fluxes separately.

During the night, when assimilation stops, the contribution of the respiration tracer to the total ${\rm CO_2}$ mixing ratio becomes large compared to the contribution of the assimilation tracers. Potentially, nocturnal mixing ratios will be able to provide us therefore with a constraint on the division between respiration and assimilation (Ahmadov et al., 2009).

However, simulation of the nocturnal PBL is an important and long known source of uncertainty (e.g. Geels et al., 2007). The stability of the atmosphere at clear nights was systematically underestimated in our simulations which will lead to biased CO_2 mixing ratio estimates. Before simulated nocturnal CO_2 mixing ratios can be used in inversion studies they must at least be corrected for the PBL height. More importantly, the simulation of the nocturnal PBL should be improved as indicated for example by Steeneveld et al. (2008). The ability of the simulations to capture variations in the atmospheric stability at small temporal scales is promising. Because of the potential high value of the nocturnal mixing ratios in separating assimilation and respiration fluxes we plan to focus more work on this issue in the future.

Summarizing, the influence of the surface CO_2 and energy fluxes on the simulated atmospheric CO_2 mixing ratio, the temperature and humidity is large, especially at days with a continental footprint. This shows that atmospheric observations potentially contain much information about these fluxes at the scale of our simulation, i.e. at a spatial scale of tens to hundreds of kilometres. Most of the variability in the CO_2 mixing ratio is caused by fluxes within the domain, mainly by biospheric fluxes. Also the fossil fuel CO_2 fluxes play a role and their uncertainty should be taken into account in inversions for such an urbanized and industrialized area. Difficulties identified in the simulation of CO_2 mixing ratios that reduce the information content of the simulated mixing ratio are (a) the systematic underestimation of the stability of the nocturnal PBL at clear nights which may lead to a biased CO_2 estimate, (b) incorrect timing of cloud formation, (c) uncertainty in the diurnal PBL height due to uncertainties in the parameterization of vertical transport and (d) the uncertainties in the driving of the atmospheric mixing by the surface energy fluxes. We quantified the latter and show it is with ~ 1.7 ppm an im-

5911

portant source of uncertainty in the CO_2 mixing ratio in the afternoon well-mixed PBL. Besides these shortcomings the atmospheric mesoscale simulation was shown to simulate the meteorological situation over the Netherlands non-stop for three weeks with reasonable accuracy. This, combined with the large simulated range of atmospheric CO_2 mixing ratios due to the spread in the CO_2 flux parameter settings provides a promising starting point for future inversion studies at the mesoscale.

Acknowledgements. This work has been executed in the framework of the Dutch project "Climate changes Spatial Planning", BSIK-ME2 and the Carboeurope Regional Component (GOCE CT2003 505572). We gratefully acknowledge the researchers who carried out measurements in the BSIK and CarboEurope consortia, with special thanks to A. Moene for providing the scintillometer data, F. Bosveld and H. Klein Baltink for the meteorological data, and E. Moors, J. Elbers, W. Jans, D. Hendriks, M. Aubinet, B. Heinesch, L. Francois and M. Carnol for the eddy correlation observations. ECMWF is acknowledged for providing meteorological observational and analysis data. Further, we would like to thank J. Vila for helpful discussions and H. ter Maat for his contribution to the RAMS simulations.

References

Ahmadov, R., Gerbig, C., Kretschmer, R., Krner, S., Rödenbeck, C., Bousquet, P., and Ramonet, M.: Comparing high resolution WRF-VPRM simulations and two global CO₂ transport models with coastal tower measurements of CO₂, Biogeosciences, 6, 807–817, 2009, http://www.biogeosciences.net/6/807/2009/.

Aubinet, M., Chermanne, B., Vandenhaute, M., Longdoz, B., Yernaux, M., and Laitat, E.: Long term carbon dioxide exchange above a mixed forest in the Belgian Ardennes, Agr. Forest Meteorol., 108(4), 293–315, 2001.

Aubinet, M., Moureaux, C., Bodson, B., Dufranne, D., Heinesch, B., Suleau, M., Vancutsem, F., and Vilret, A.: Carbon sequestration by a crop over a 4-year sugar beet/winter wheat/seed potato/winter wheat rotation cycle, Agr. Forest Meteorol., 149(3–4), 407–418, 2009.

Baldocchi, D., Falge, E., Gu, L. H., Olson, R., Hollinger, D., Running, S., Anthoni, P., Bernhofer, C., Davis, K., Evans, R., Fuentes, J., Goldstein, A., Katul, G., Law, B., Lee, X. H., Malhi, Y., Meyers, T., Munger, W., Oechel, W., U, K. T. P., Pilegaard, K., Schmid, H. P., Valentini,

- R., Verma, S., Vesala, T., Wilson, K., and Wofsy, S.: FLUXNET: A new tool to study the temporal and spatial variability of ecosystem-scale carbon dioxide, water vapor, and energy flux densities, B. Am. Meteorol. Soc., 82(11), 2415–2434, 2001.
- Bosveld, F. C., De Bruijn, E. I. F., and Holtslag, A. A. M.: Intercomparison of single-coumn models for GABLS3: preliminary results, AMS, 18th Symposium on Boundary Layers and Turbulence, 2008.
 - Braam, M.: Determination of the surface sensible heat flux from the structure parameter of temperature at 60 m height during daytime, KNMI TR-303, De Bilt, 36 pp., 2008.
- Canadell, J. G., Le Quéré, C., Raupach, M. R., Field, C. B., Buitenhuis, E. T., Ciais, P., Conway, T. J., Gillett, N. P., Houghton, R. A., and Marland, G.: Contributions to accelerating atmospheric CO₂ growth from economic activity, carbon intensity, and efficiency of natural sinks, P. Natl. Acad. Sci., 104(47), 18866–18870, 2007.
- Casso-Torralba, P., Vila-Guerau De Arellano, J. V. G., Bosveld, F. C., Soler, M. R., Vermeulen, A. T., Werner, C., and Moors, E. J.: Diurnal and vertical variability of the sensible heat and carbon dioxide budgets in the atmospheric surface layer, J. Geophys. Res.-Atmos., 113(D12), D12119, doi:10.1029/2007JD009583, 2008.
- Collatz, G. J., Ball, J. T., Grivet, C., and Berry, J. A.: Physiological and Environmental-Regulation of Stomatal Conductance, Photosynthesis and Transpiration a Model That Includes a Laminar Boundary-Layer, Agr. Forest Meteorol., 54(2–4), 107–136, 1991.
- Corbin, K. D., Denning, A. S., Lu, L., Wang, J. W., and Baker, I. T.: Possible representation errors in inversions of satellite CO₂ retrievals, J. Geophys. Res.-Atmos., 113(D2), D02301, doi:10.1029/2007JD008716, 2008.
 - De Bruin, H. A. R., Moene, A. F., and Bosveld, F. C.: An Integrated MSG-Scintillometer network system to monitor sensible and latent heat fluxes, in: Proc. 2nd MSG RAO Workshop (ESA SP-582), edited by: Lacoste, H., 137–142, 2004.
 - Denning, A. S., Nicholls, M., Prihodko, L., Baker, I., Vidale, P. L., Davis, K., and Bakwin, P.: Simulated variations in atmospheric CO₂ over a Wisconsin forest using a coupled ecosystem-atmosphere model, Glob. Change Biol., 9(9), 1241–1250. 2003.
- Dolman, A. J., Moors, E. J., and Elbers, J. A.: The carbon uptake of a mid latitude pine forest growing on sandy soil, Agr. Forest Meteorol., 111(3), 57–170, 2002.
- Dolman, A. J., Noilhan, J., Durand, P., Sarrat, C., Brut, A., Piguet, B., Butet, A., Jarosz, N., Brunet, Y., Loustau, D., Lamaud, E., Tolk, L., Ronda, R., Miglietta, F., Gioli, B., Magliulo, V., Esposito, M., Gerbig, C., Korner, S., Glademard, R., Ramonet, M., Ciais, P., Neininger, B.,

- Hutjes, R. W. A., Elbers, J. A., Macatangay, R., Schrems, O., Perez-Landa, G., Sanz, M. J., Scholz, Y., Facon, G., Ceschia, E., and Beziat, P.: The CarboEurope regional experiment strategy, B. Am. Meteorol. Soc., 87(10), 1367–1379, 2006.
- Ek, M. B. and Holtslag, A. A. M.: Influence of soil moisture on boundary layer cloud development, J. Hydrometeorology, 5(1), 86–99, 2004.
- Farquhar, G. D., Caemmerer, S. V., and Berry, J. A.: A biochemical model of photosynthetic CO₂ assimilation in leaves of C3 species, Planta, 149(1), 78–90, 1980.
- Geels, C., Gloor, M., Ciais, P., Bousquet, P., Peylin, P., Vermeulen, A. T., Dargaville, R., Aalto, T., Brandt, J., Christensen, J. H., Frohn, L. M., Haszpra, L., Karstens, U., Rödenbeck, C., Ramonet, M., Carboni, G., and Santaguida, R.: Comparing atmospheric transport models for future regional inversions over Europe Part 1: mapping the atmospheric CO₂ signals, Atmos. Chem. Phys., 7, 3461–3479, 2007, http://www.atmos-chem-phys.net/7/3461/2007/.
- Gerbig, C., Körner, S., and Lin, J. C.: Vertical mixing in atmospheric tracer transport models: error characterization and propagation, Atmos. Chem. Phys., 8, 591–602, 2008, http://www.atmos-chem-phys.net/8/591/2008/.
 - Gerbig, C., Dolman, A. J., and Heimann, M.: On observational and modelling strategies targeted at regional carbon exchange over continents, Biogeosciences Discuss., 6, 1317–1343, 2009.
- http://www.biogeosciences-discuss.net/6/1317/2009/.
- Groenendijk, M., van der Molen, M. K., and Dolman, A. J.: Seasonal variation in ecosystem parameters derived from FLUXNET data, Biogeosciences Discuss., 6, 2863–2912, 2009, http://www.biogeosciences-discuss.net/6/2863/2009/.
- Gurney, K. R., Law, R. M., Denning, A. S., Rayner, P. J., Baker, D., Bousquet, P., Bruhwiler, L., Chen, Y. H., Ciais, P., Fan, S., Fung, I. Y., Gloor, M., Heimann, M., Higuchi, K., John, J., Maki, T., Maksyutov, S., Masarie, K., Peylin, P., Prather, M., Pak, B. C., Randerson, J., Sarmiento, J., Taguchi, S., Takahashi, T., and Yuen, C. W.: Towards robust regional estimates of CO₂ sources and sinks using atmospheric transport models, Nature, 415(6872), 626–630, 2002.
- Holtslag, A. A. M., Meijgaard, E., and Rooy, W. C.: A comparison of boundary layer diffusion schemes in unstable conditions over land, Bound.-Lay. Meteorol., 76(1), 69–95, 1995.
- Hong, S. Y. and Pan, H. L.: Nonlocal boundary layer vertical diffusion in a medium-range forecast model, Mon. Weather Rev., 124(10), 2322–2339, 1996.
- Jacobs, C. M. J., Jacobs, A. F. G., Bosveld, F. C., Hendriks, D. M. D., Hensen, A., Kroon, P.

- S., Moors, E. J., Nol, L., Schrier-Uijl, A., and Veenendaal, E. M.: Variability of annual $\rm CO_2$ exchange from Dutch grasslands, Biogeosciences, 4, 803–816, 2007, http://www.biogeosciences.net/4/803/2007/.
- Lauvaux, T., Uliasz, M., Sarrat, C., Chevallier, F., Bousquet, P., Lac, C., Davis, K. J., Ciais, P., Denning, A. S., and Rayner, P. J.: Mesoscale inversion: first results from the CERES campaign with synthetic data, Atmos. Chem. Phys., 8, 3459–3471, 2008, http://www.atmos-chem-phys.net/8/3459/2008/.
- Law, R. M., Peters, W., Rödenbeck, C., Aulagnier, C., Baker, I. T., Bergmann, D. J., Bousquet, P., Brandt, J., Bruhwiler, L., and Cameron-Smith, P. J.: TransCom model simulations of hourly atmospheric CO₂: Experimental overview and diurnal cycle results for 2002, Global Biogeochem. Cy., 22, GB3009, doi:10.1029/2007GB003050, 2008.
- Lin, J. C. and Gerbig, C.: Accounting for the effect of transport errors on tracer inversions, Geophys. Res. Lett., 32, L01802, doi:10.1029/2004GL021127, 2005.
- Lloyd, J. and Taylor, J. A.: On the temperature dependence of soil respiration, Funct. Ecol., 8, 315–323, 1994.
- Medvigy, D., Moorcroft, P. R., Avissar, R., and Walko, R. L.: Mass conservation and atmospheric dynamics in the regional atmospheric modeling system (RAMS), Environ. Fluid Mech., 5(1–2), 109–134, 2005.
- Meesters, A. G. C. A., Tolk, L. F., and Dolman, A. J.: Mass conservation above slopes in the Regional Atmospheric Modelling System (RAMS), Environ. Fluid Mech., 8(3), 239–248, 2008.
 - Nicholls, M. E., Denning, A. S., Prihodko, L., Vidale, P. L., Baker, I., Davis, K., and Bakwin, P.: A multiple-scale simulation of variations in atmospheric carbon dioxide using a coupled biosphere-atmospheric model, J. Geophys. Res.-Atmos., 109(D18), D18117, doi:10.1029/2003JD004482, 2004.
 - Parazoo, N. C., Denning, A. S., Kawa, S. R., Corbin, K. D., Lokupitiya, R. S., and Baker, I. T.: Mechanisms for synoptic variations of atmospheric CO₂ in North America, South America and Europe, Atmos. Chem. Phys., 8, 7239–7254, 2008, http://www.atmos-chem-phys.net/8/7239/2008/.
- Peters, W., Jacobson, A. R., Sweeney, C., Andrews, A. E., Conway, T. J., Masarie, K., Miller, J. B., Bruhwiler, L. M. P., Pétron, G., and Hirsch, A. I.: An atmospheric perspective on North American carbon dioxide exchange: CarbonTracker, P. Natl. Acad. Sci. USA, 104(48), 18925–18930, 2007.

- Pielke, R. A., Cotton, W. R., Walko, R. L., Tremback, C. J., Lyons, W. A., Grasso, L. D., Nicholls, M. E., Moran, M. D., Wesley, D. A., Lee, T. J., and Copeland, J. H.: A Comprehensive Meteorological Modeling System –RAMS, Meteorol. Atmos. Phys., 49(1–4), 69–91, 1992.
- Riley, W. J., Randerson, J. T., Foster, P. N., and Lueker, T. J.: Influence of terrestrial ecosystems and topography on coastal CO₂measurements: A case study at Trinidad Head, California, J. Geophys. Res.-Biogeos., 110(G1), G01005, doi:10.1029/2004JG000007, 2005.
- Sarrat, C., Noilhan, J., Dolman, A. J., Gerbig, C., Ahmadov, R., Tolk, L. F., Meesters, A. G. C. A., Hutjes, R. W. A., Ter Maat, H. W., Pérez-Landa, G., and Donier, S.: Atmospheric CO₂ modeling at the regional scale: an intercomparison of 5 meso-scale atmospheric models, Biogeosciences, 4, 1115–1126, 2007,
- http://www.biogeosciences.net/4/1115/2007/.
- Sellers, P. J., Los, S. O., Tucker, C. J., Justice, C. O., Dazlich, D. A., Collatz, G. J., and Randall, D. A.: A revised land surface parameterization (SiB2) for atmospheric GCMs. Part II: The generation of global fields of terrestrial biophysical parameters from satellite data, J. Climate, 9(4), 706–737, 1996.
- Skamarock, W. C. and Klemp, J. B.: A time-split nonhydrostatic atmospheric model for weather research and forecasting applications, J. Comp. Phys., 227(7), 3465–3485, 2008.
- Steeneveld, G. J., Mauritsen, T., De Bruijn, E. I. F., Vilà-Guerau De Arellano, J., Svensson, G., and Holtslag, A. A. M.: Evaluation of limited-area models for the representation of the diurnal cycle and contrasting nights in CASES-99, J. Appl. Meteorol. Clim., 47(3), 869–887, 2008.
- Stephens, B. B., Gurney, K. R., Tans, P. P., Sweeney, C., Peters, W., Bruhwiler, L., Ciais, P., Ramonet, M., Bousquet, P., and Nakazawa, T.: Weak northern and strong tropical land carbon uptake from vertical profiles of atmospheric CO₂, Science, 316(5832), 1732–1735, 2007.
- Takahashi, T., Sutherland, S. C., Sweeney, C., Poisson, A., Metzl, N., Tilbrook, B., Bates, N., Wanninkhof, R., Feely, R. A., and Sabine, C.: Global sea-air CO₂ flux based on climatological surface ocean pCO₂, and seasonal biological and temperature effects, Deep-Sea Res. Pt II, 49(9–10), 1601–1622, 2002.
- Ter Maat, H. W. and Hutjes, R. W. A.: Simulating carbon exchange using a regional atmospheric model coupled to an advanced land-surface model, Biogeosciences Discuss., 5, 4161–4207, 2008,
 - http://www.biogeosciences-discuss.net/5/4161/2008/.
 - Tolk, L. F., Meesters, A. G. C. A., Dolman, A. J., and Peters, W.: Modelling representation errors

- of atmospheric CO2 mixing ratios at a regional scale, Atmos. Chem. Phys., 8, 6587–6596, 2008.
- http://www.atmos-chem-phys.net/8/6587/2008/.
- Troen, I. B. and Mahrt, L.: A simple model of the atmospheric boundary layer; sensitivity to surface evaporation, Bound.-Lay. Meteorol., 37(1), 129–148, 1986.
- Uppala, S. M., Kallberg, P. W., Simmons, A. J., Andrae, U., Bechtold, V. D., Fiorino, M., Gibson, J. K., Haseler, J., Hernandez, A., Kelly, G. A., Li, X., Onogi, K., Saarinen, S., Sokka, N., Allan, R. P., Andersson, E., Arpe, K., Balmaseda, M. A., Beljaars, A. C. M., Van De Berg, L., Bidlot, J., Bormann, N., Caires, S., Chevallier, F., Dethof, A., Dragosavac, M., Fisher, M.,
- Fuentes, M., Hagemann, S., Holm, E., Hoskins, B. J., Isaksen, L., Janssen, P., Jenne, R., Mcnally, A. P., Mahfouf, J. F., Morcrette, J. J., Rayner, N. A., Saunders, R. W., Simon, P., Sterl, A., Trenberth, K. E., Untch, A., Vasiljevic, D., Viterbo, P., and Woollen, J.: The ERA-40 re-analysis, Q. J. Roy. Meteor. Soc., 131(612), 2961–3012, 2005.
- Van Der Molen, M. K. and Dolman, A. J.: Regional carbon fluxes and the effect of topography on the variability of atmospheric CO₂, J. Geophys. Res.-Atmos., 112(D1), D01104, doi:10.1029/2006JD007649, 2007.
 - Van Lipzig, N. P. M., Schröder, M., Crewell, S., Ament, F., Chaboureau, J. P., Löhnert, U., Matthias, V., Van Meijgaard, E., Quante, M., and Willén, U.: Model predicted low-level cloud parameters Part I: Comparison with observations from the BALTEX Bridge Campaigns, Atmos. Res., 82(1–2), 55–82, 2006.
 - Vila-Guerau De Arellano, J. V. G., Gioli, B., Miglietta, F., Jonker, H. J. J., Baltink, H. K., Hutjes, R. W. A., and Holtslag, A. A. M.: Entrainment process of carbon dioxide in the atmospheric boundary layer, J. Geophys. Res., 109, D18110, doi:10.1029/2004JD004725, 2004.
- Vila-Guerau De Arellano, V. G. and Casso-Torralba, P.: The radiation and energy budget in mesoscale models, Física de la tierra, 19, 117–132, 2007.
 - Walko, R. L., Band, L. E., Baron, J., Kittel, T. G. F., Lammers, R., Lee, T. J., Ojima, D., Pielke, R. A., Taylor, C., Tague, C., Tremback, C. J., and Vidale, P. L.: Coupled atmosphere-biophysics-hydrology models for environmental modeling, J. Appl. Meteorol., 39(6), 931–944, 2000.
- Wanninkhof, R.: Relationship between Wind-Speed and Gas-Exchange over the Ocean, J. Geophys. Res.-Oceans, 97(C5), 7373–7382, 1992.
- Wilson, K., Goldstein, A., Falge, E., Aubinet, M., Baldocchi, D., Berbigier, P., Bernhofer, C., Ceulemans, R., Dolman, H., and Field, C.: Energy balance closure at FLUXNET sites, Agr. Forest Meteorol., 113(1–4), 223–243, 2002.

Zupanski, D., Denning, A. S., Uliasz, M., Zupanski, M., Schuh, A. E., Rayner, P. J., Peters, W., and Corbin, K. D.: Carbon flux bias estimation employing maximum likelihood ensemble filter (MLEF), J. Geophys. Res., 112, D17107, doi:10.1029/2006JD008371, 2007.

Table 1. Specification of the simulation settings.

Simulation Specifications	
Atmospheric model Vegetation model CO ₂ flux model Turbulence scheme	Brams-3.2 Leaf-3 5PM MRF
Simulation setup	
Nesting Domain, resolution	Two way nested 320×320 km, 4 km 640×640 km, 16 km 40 levels (23 in lower 2 km)
Domain centre	52.25° N, 5.2° E
Initial & boundary conditions	
Soil moisture and Temperature CO ₂ concentration Meteorology	ECMWF analysis data (www.ecmwf.int) 3 hourly nudged to CarbonTracker 1×1° 6 hourly nudged to ECMWF analysis
Surface Characteristics	
Land use Topography Soil textural class Fossil fuel emissions	Pelcom dataset (http://www.geo-informatie.nl/projects/pelcom/) USGS dataset (www.atmet.com) UN FAO dataset (www.atmet.com) IER database (http://carboeurope.ier.uni-stuttgart.de)

Table 2. CO_2 flux parameter settings based on Groenendijk et al. (2009). Vc_{max} is the full canopy maximum carboxylation capacity, α the light use efficiency for the full canopy, E_0/\Re is the respiration activation energy divided by the universal gas constant, R_{10} is the respiration rate at 10°C and n sites indicates the number of sites used in the optimizations of the parameters. Where uncertainty ranges are shown the best guess, upper and lower estimates of the parameters are used in the simulations. In between brackets the parameter values that returned the best CO_2 mixing ratios.

Assimilation			
	$Vc_{\text{max}} (\mu \text{mol m}^{-2} \text{ s}^{-1})$	$\alpha \text{ (mol mol}^{-1})$	n sites
Grass	70±30 (40)	0.4±0.15 (0.4)	10
Crops	100±50 (100)	$0.4\pm0.15(0.4)$	5
Needle leaf forest	80	0.5	10
Broadleaf forest	100	0.5	2
Urban vegetation	80	0.4	_
Respiration			
	E ₀ /ℜ (K)	$R_{10} (\mu \text{mol m}^{-2} \text{s}^{-1})$	n sites
Full domain	200±110 (310)	4.6±1.2 (3.5)	10

Table 3. Observation specifications. EC is eddy correlation measurements, Sc is scintillometer, RS is radiosonde and TT is tall tower.

Site name	Vegetation type	Longitude	Latitude	Observation	Data providers
Cabauw (Ca1)	Grass	4.93	51.97	EC TT CO ₂ TT meteo	www.carboeurope.org A. Vermeulen; ECN F. Bosveld, H. Klein Baltink; KNMI
De Bilt	Grass, forest, urban	5.18	52.1	RS	F. Bosveld, H. Klein Baltink; KNMI
Haarweg (Haa)	Grass	5.63	51.97	EC	www.carboeurope.org
• ,				Sc	A. Moene; Wageningen University
Horstermeer (Hor)	Grass	5.04	52.14	EC	www.carboeurope.org
Lonzee (Lon)	Crops	4.75	50.55	EC	www.carboeurope.org
Loobos (Loo)	Needle Forest	5.74	52.17	EC	www.carboeurope.org
Lutjewad (Lut)	Crops	6.37	53.38	EC	www.carboeurope.org
Maas en Waal (MeW)	Crops, grass, trees	5.7	51.82	Sc	A. Moene; Wageningen University

Table 4. Statistics of the simulation, in comparison with observations of the potential temperature (T) and CO_2 at 20m and 200m, humidity (q) at 2m and the incoming shortwave radiation (rshort) at Cabauw, for the full period, the first and the second half of the simulation period. Humidity is compared to the simulated canopy air humidity, CO_2 and T with simulated atmospheric values.

	F	ull period		First half	Second half		
	R^2	RMSE	R^2	RMSE	R^2	RMSE	
T 200 m	0.90	1.2 K	0.92	1.2 K	0.87	1.1 K	
T 20 m	0.87	1.4 K	0.92	1.3 K	0.80	1.5 K	
q 2 m	0.51	1.1 g kg ⁻¹	0.47	$1.3\mathrm{gkg}^{-1}$	0.65	$0.8\mathrm{gkg}^{-1}$	
Rshort	0.78	$143.4\mathrm{Wm^{-2}}$	0.88	$113.2\mathrm{Wm^{-2}}$	0.64	$165.6\mathrm{Wm^{-2}}$	
CO ₂ 200 m	0.21	5.9 ppm	0.15	5.8 ppm	0.23	6.3 ppm	
CO ₂ 20 m	0.67	10.1 ppm	0.71	11.0 ppm	0.55	9.8 ppm	

Table 5. Overview of the sensitivity tests. Results are given for 11 June 12:00. Simulation settings: Pre-sim is the time simulated before this moment, SM is the soil moisture content, rs_{\min} is the minimal stomatal resistance of the low vegetation, veg. frac. is the vegetation fraction. Results: Bowen ratio (β) , sensible (H) and latent (LE) heat flux, all for Cabauw; and observed potential temperature (T) for De Bilt at 500 m height (radiosonde observation), and its difference (Tsim-Tobs) with the simulated value. Sim. ID identifies the two simulations further used in this study (for more information see the text). The grey blocks indicate the change compared to the preceding simulation.

Observed				β	Н	LE	T	
				0.13	62.9	480	24.7	
Simulated								
Pre-sim.	SM	rs _{min}	veg. frac.	β	Н	LE	$T_{\rm obs}$ - $T_{\rm sim}$	Sim. ID
days	$\mathrm{m}^{3}\mathrm{m}^{-3}$	s/m	%	-	W/m ²	W/m ²	K	
5.75	0.23	100	70	0.17	70	408	3.1	low β
0.75	0.23	100	70	0.17	72	423	2.5	
0.25	0.23	100	70	0.16	70	447	2	
0.25	0.19	100	70	0.30	113	380	1.1	
0.25	0.23	200	70	0.27	106	389	1.5	
0.25	0.23	200	90	0.29	128	441	0.9	high $oldsymbol{eta}$

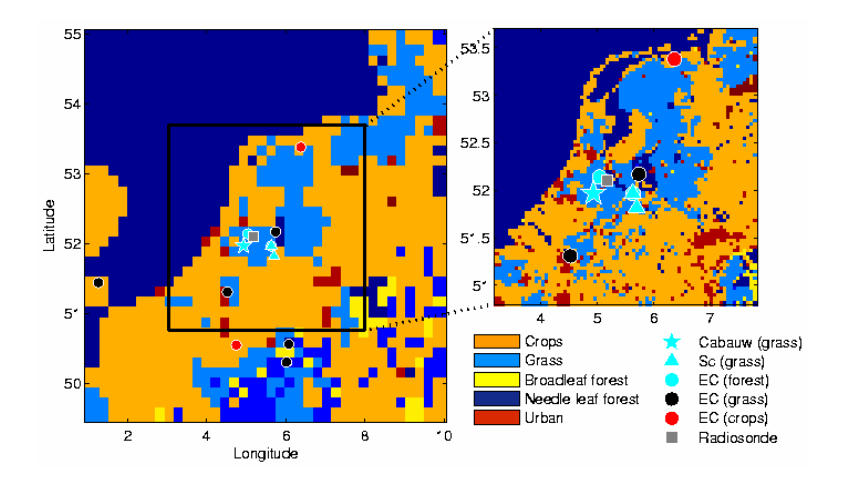


Fig. 1. Simulation domain with 2 nested grids. The star indicates Cabauw, the square the location of the radiosonde release, the triangles indicate the scintillometers and the dots the eddy correlation observations.

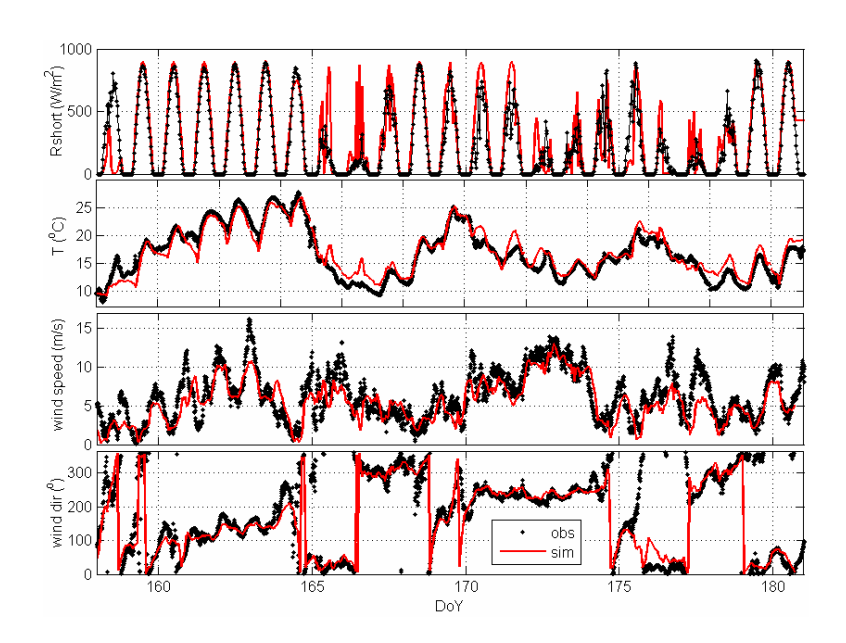


Fig. 2. Observed and simulated time series at the Cabauw of (a) short wave radiation, (b) potential temperature, (c) wind speed and (d) wind direction at 200 m.

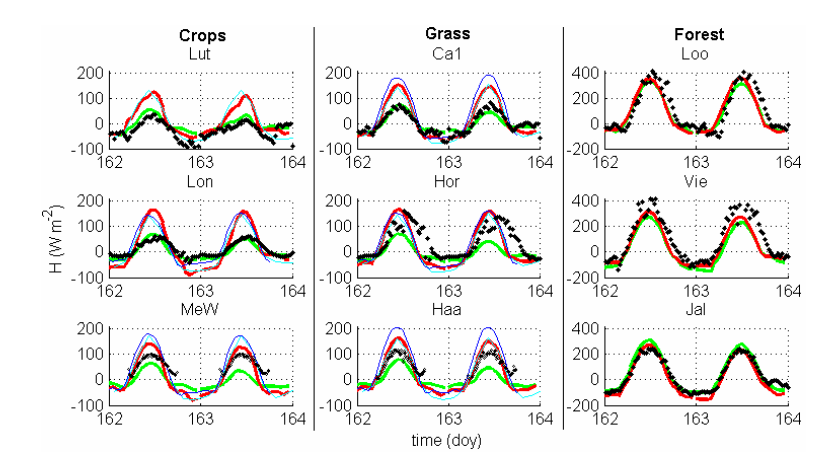


Fig. 3. Sensible heat flux for crops, grasslands and forest at 11 and 12 June 2006 (doy 162 and 163), for locations and full names see Table 3. The black dots indicate for Maas en Waal (MeW) and Haarweg (Haa) scintillometer observations and for the other sites eddy correlation observations. Green indicates the RAMS simulation with a low Bowen ratio, and red with a high Bowen ratio (see text for explanation), dark blue is the WRF simulation and light blue is the ECMWF forecast simulation.

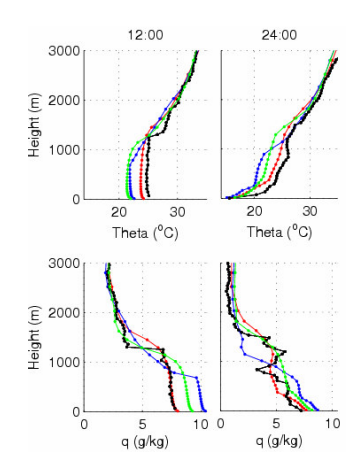


Fig. 4. Simulated and observed potential temperature and humidity profiles at De Bilt, 11 June 2006, at 12:00 (left) and 24:00 (right). Black indicates the radiosonde observations, red the simulation with a high Bowen ratio, green the simulation with a low Bowen ratio. Blue indicates the simulation with a low Bowen ratio, but with the Mellor Yamada instead of MRF turbulence scheme.

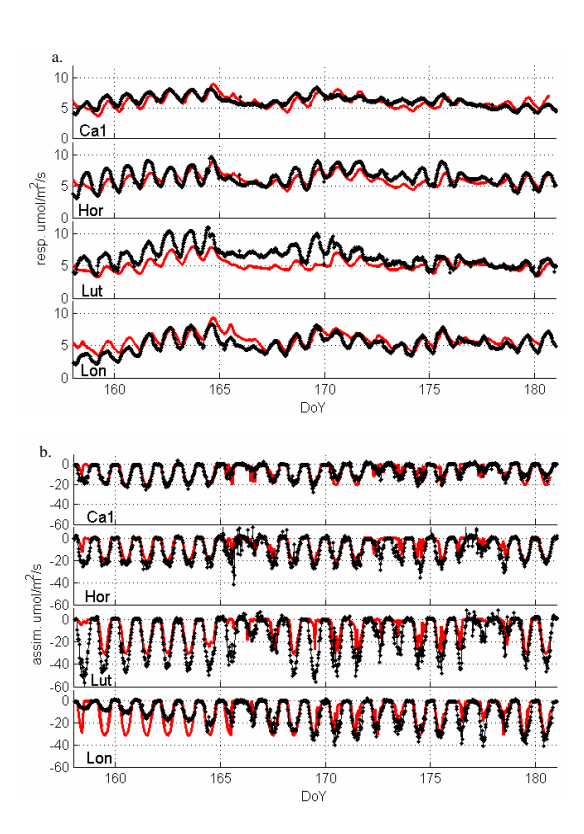


Fig. 5. Simulated (red) and observed (black) respiration (a) and assimilation (b) fluxes, showing the difference in CO_2 fluxes observed between sites and the ability of the model to simulate these with CO_2 flux parameters that return unbiased CO_2 mixing ratios.

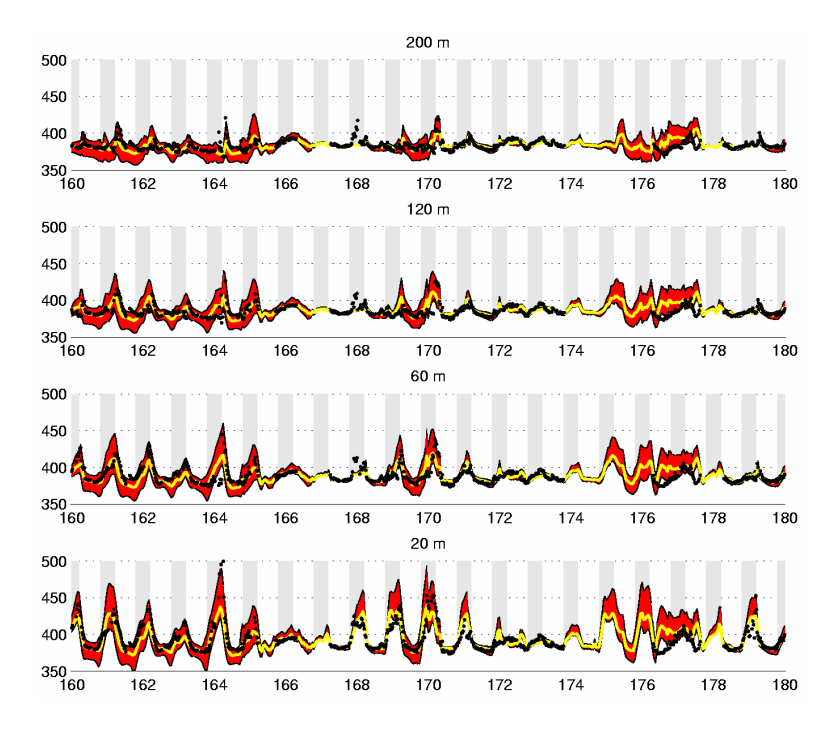


Fig. 6. CO_2 concentration at 4 heights at Cabauw tower. In black the observations. The red band is the range of CO_2 mixing ratio simulated with a spread of CO_2 flux parameters (table 2), it reflects the effect of uncertainties in the surface CO_2 fluxes on the CO_2 mixing ratios. Yellow shows the simulation that best fits the observations.

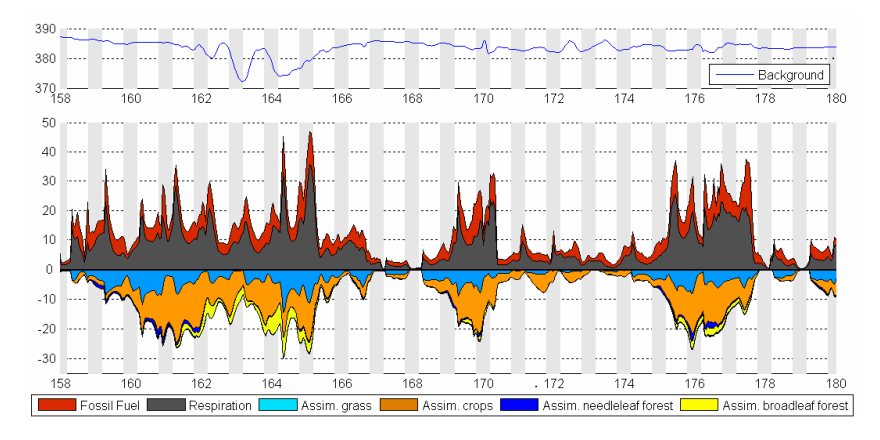


Fig. 7. Contribution of the background CO_2 to the mixing ratio at Cabauw 200 m (a) and the cumulative contribution of the CO_2 fluxes in the domain (b). The variation in the CO_2 mixing ratio is mainly determined by the fossil fuel, respiration and assimilation fluxes, where atmospheric signal from assimilation by crops dominates over grass assimilation.

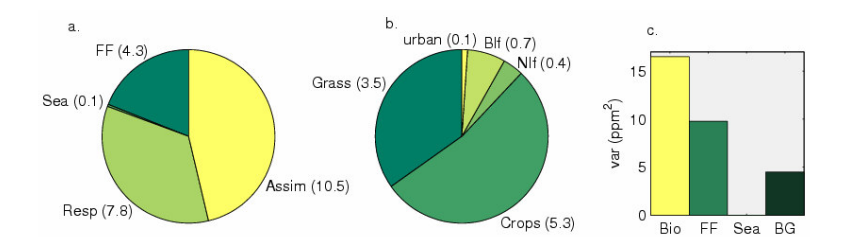


Fig. 8. Average contribution of the different tracers to the diurnal CO_2 mixing ratio (a and b) and its variance (c) at 200 m at Cabauw. (a) shows the influence of the assimilation (assim), respiration (resp), sea and fossil fuel (FF) fluxes. In (b) the assimilation flux influence is separated by vegetation type: urban vegetation, broadleaf forest (Blf), needle leaf forest (Nlf), crops and grass. In (c) the variability is shown which is due to variations in the biospheric (bio), fossil fuel (FF), and sea fluxes, and in the background mixing ratio (BG).